SLAG CONTROL FOR SULPHUR REDUCTION IN A STAINLESS STEEL MAKING PROCESS

Neil Sutcliffe[1] and Robert C. Nunnington[2]
[1] Columbus Joint Venture, trading as Columbus Stainless, sutcliffe.neil@columbus.co.za
[2] Formerly with Columbus Stainless, now Baker Refractories, rnunnington@bakerref.com

---

ABSTRACT

The effective control of slag chemistry during the decarburisation and reduction stages of stainless steel manufacturing in a CLU converter, allows for sulphur removal down to 0.003 wt%, with a single slag practice. Subsequent use of a high-basicity synthetic slag practice at the rinsing station allows the attainment of sulphur levels down to 0.001 wt%. This paper presents the strategies followed, and addition practices utilised, to achieve these results. The validation of published sulphur distribution calculations is presented and their applicability to the plant environment is discussed.

1. Introduction

In this paper, the effective control of sulphur in stainless steel production will be discussed from the perspective of slag chemistry control and additions practices at various stages in the process. The applicability of published sulphur distribution ratios to the steelmaking at Columbus Stainless will be discussed. The customer requirements for decreased sulphur contents in stainless steels and the market forces necessitating increased production levels require the application of a single slag practice, which accurately control the sulphur level, does not increase the cost of production or increase the processing time. It is from this perspective that the slag practices at the EAF, CLU and Rinsing Station are designed.

2. Theoretical Background

Researchers have proposed various methods for the prediction and control of sulphur behaviour in stainless steel slag and metal systems. These include the classic Optical Basicity approach of Sosinsky and Sommerville [1], the modified Optical basicity approach of Duffy[2] and the use of measured sulphide capacities, together with the prediction of oxygen potential, based on measured activity data for slags and alloys. The third approach has received the most attention and development, based on its applicability to any system that is adequately described by experimental data, and that it does not require sophisticated models or software.

Optical Basicity values are calculated based on the Pauling Electronegativity of an oxide species in a slag. Sosinsky and Sommerville [1] compared the Optical Basicity of various slag systems with the sulphide capacity of these systems, and applied a linear regression to the data to give an empirical prediction of the sulphide capacity for any slag system. Their equation is given below:

$$LogC_{S1} = \frac{(22690 - 54640\Lambda)}{T} + 43.6\Lambda - 25.2 \qquad (1)$$

(Note on symbols: ( ) references the slag species, [ ] references metal species, Λ = Optical Basicity, T is temperature in Kelvin unless otherwise stated.)

The Optical Basicity, Λ, is a composite of the optical basicity values for each oxide component of the slags being investigated, e.g. Λ_{MgO}, Λ_{CaO} etc.

Work by various authors[2,3] has indicated that the linear approximation approach of the Optical Basicity method, does not accurately predict sulphide capacity behaviour at high and low levels of sulphide capacity. The effects of CaF_2 are also not considered by equation 1, which has lead to the modified approach of Duffy[2]. The following equation is a regression of the data referenced and generated in their paper.

$$LogC_{S2} = -15.2424 + 23.1128\Lambda_{mod} - \frac{8992\Lambda_{mod}}{T} + 5.0556N_{CaF_2} \qquad (2)$$

where, Λ_{mod} = modified optical basicity[2]
N_{CaF2} = mole fraction of CaF_2

The utilisation of equations 1 and 2 in a plant situation are discussed later.

Calculation Approach using Thermodynamic data and measured C_S data

The basic definition of the sulphide capacity may be developed as follows:

$$C_S = (wt\%S)\sqrt{\frac{P_{O_2}}{P_{S_2}}} \qquad (3)^{[4]}$$

where P_{O2} and P_{S2} are the partial pressures of oxygen and sulphur gases present, in equilibrium with the slag phase. For the case of the slag-metal reaction, P_{O2} and P_{S2} are related to the activities of oxygen and sulphur in the metal through the following reactions, where K_4 and K_5 are the equilibrium constants of reactions 4 and 5.

$$\frac{1}{2}(O_2) = [O] \qquad (4)$$

ΔG_4^o = - 117000 - 2.9T [J/Mol] [5].

$$\frac{1}{2}S_2 = [S] \qquad (5)$$

ΔG_5^0 = - 135100 – 23.4T [J/Mol] [5]

The sulphur partition ratio, $\mathbf{L}_S$, is related to the sulphide capacity by the following relationship:

$$L_S = \frac{(\%S)}{[\%S]} = C_S \frac{f_S \cdot K_4}{a_O \cdot K_5} \qquad (6)$$

From the above definition, it can be seen that the sulphur capacity of a slag is a function of measurable and calculable values. The critical areas of the above definition are the activity

coefficient of sulphur in the steel, C_S and the reaction controlling sulphur removal. Appendix 1 lists and references the data used to calculate the activity coefficients utilised in this work for the important species in the steel.

Sulphur Removal Reaction

In general terms, the sulphur removal reaction can be based on Al or Si controlling the oxygen potential in the steel:

$$2[Al] + 3[O] = Al_2O_{3(s)} \tag{7}$$
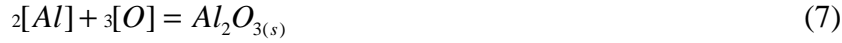
$$\Delta G_{Al}^{\ 0} = -1202000 + 386.3T \qquad \text{(Ref. 5)}$$

Which allows the sulphide capacity, C_S to be defined as follows[5]:

$$C_S = \frac{(\% S) \cdot a_{Al_2O_3}^{1/3}}{f_{[Al]}^{2/3} \cdot [\% Al]^{2/3} \cdot f_{[S]} \cdot [\% S]} \cdot \frac{K_5}{K_7^{1/3} \cdot K_4} \tag{8}$$

For Si control:

$$[Si] + 2O = SiO_2 \tag{9}$$

$$\Delta G_9^0 = -570603 + 21.586T \ ^{(6)}$$

Leading to

$$C_S = \frac{(\% S) \cdot a_{SiO_2}^{1/2} \cdot K_5}{f_{Si}^{1/2} \cdot [\% Si]^{1/2} \cdot K_9 \cdot f_S \cdot [\% S]} \tag{10}$$

The underlying oxygen equilibrium utilised in the above equations is for oxygen in the bulk metal [O]. However, Jonsson et al[7], utilising CFD and thermodynamic modelling, and Inoue and Suito [5] indicated that the equilibrium oxygen is controlled by the [Al]/(Al$_2$O$_3$) at the slag metal interface or mixing zone, where sufficient [Al] is present. This complicates matters considerably, as [Al] reacts with other species, such as Ca, CaO, Mg and MgO to form solid and liquid inclusions in this region, thereby modifying the final equilibrium oxygen value. Suito et al[8] have noted the supersaturation effect of [Al] at low concentrations of Al in the metal, which leads to oxygen levels higher than the equilibrium values.

In modelling complex systems, it is thus necessary to either make some simplifying assumptions, or utilise a free energy minimisation calculation approach (FEM) to cover all of the possible reactions occurring in the system.

In the current work, several assumptions have been made:
- The [%Ca] is assumed to be negligible.
- The thermodynamic data (interaction parameters) and the sources are listed in appendix 1. (The data was verified from extensive modelling work on the plant.)
- The species, either Si or Al, which controls the equilibrium oxygen level at a certain temperature and composition are calculated by means of an inclusion stability model, where the lowest oxygen potential in the steel is calculated from activity coefficient data, together with the steel and slag compositions. During the refining process of stainless steel, the temperature and composition constantly change, thus with time the controlling

species may change. This key fact necessitates the alternating use of equation sets (7 and 8) and (9 and 10) for the calculation of the sulphide capacity and thus the sulphur in the steel. Ohta and Suito's[9] approximations for the a_{SiO2} and a_{Al2O3} are used in the calculations. The approximation for both activities is extrapolated for the CLU slags at 1700 ^{o}C.

- As no direct measurements of the sulphide capacity of the slags under investigation have been made, several correlations reported in literature have been investigated. These are shown as equation 1 and 2 above and equation 11 below[10].

$$C_{S11} = 3.44\left(N_{CaO} + 0.1N_{MgO} - 0.8N_{Al_2O_3} - N_{SiO_2}\right) - \frac{9894}{T} + 2.05 \qquad (11)$$

Equations 1, 2 and 11 thus allow the definition of sulphur distribution ratios as follows:

$$LogL_{S1} = \frac{-935}{T} + 1.375 + LogC_{S1} + Logf_s - Log[a_o] \qquad (12)^{(1,11)}$$

$$LogL_{S2} = \frac{-935}{T} + 1.375 + LogC_{S2} + Logf_s - Log[a_o] \qquad (13)^{(2,11)}$$

Equation 14 is for silicon control of the oxygen potential (from equations 9 and 11) and equation 15 is for aluminium control of the oxygen potential (from equations 7 and 11).

$$LogL_{S3} = \frac{C_{S11} \cdot f_{[Si]}^{1/2} \cdot [\% Si]^{1/2} \cdot K_9 \cdot f_{[S]}}{a_{SiO_2}^{1/2} \cdot K_5} \qquad (14)$$

$$LogL_{S4} = \frac{C_{S11} \cdot f_{[Al]}^{2/3} \cdot [\% Al]^{2/3} \cdot f_{[S]} \cdot K_7^{1/3} \cdot K_4}{a_{Al_wO_3}^{1/3} \cdot K_5} \qquad (15)^{(5)}$$

The results of the application of these equations are discussed in section 4. Several other sulphur distribution ratios have been reported in literature[11,12,13,14]. These models were found to be inapplicable to the slag systems examined in this work.

3. Plant Trials
3.1 Process Description

Columbus Stainless is situated in Middelburg, South Africa. The steelmaking facilities consist of a 100t EAF (with side tapping) two stationary 100t CLU (Creusot-Loire-Uddeholm) converters (with top lance), ladle rinsing station and a straight mould, curved bow, continuous casting machine. The product range covers standard 300 and 400 grades as well as titanium-stabilised grades. The current throughput is 45 to 50 000t per month of 70% austenitic and 30% ferritic grades.

The EAF slag is balanced to protect refractories, enable reduction of Cr_2O_3 during tapping and to allow a transfer sulphur level <0.025wt%. Table 1 shows the mean slag chemistry and sulphur levels in the slag for 304-type steel. During tapping, lime and FeSi are added to the

stream to allow rapid reduction of the slag. The slag is then decanted and rabbled, achieving a slag mass of 800 to 1000Kg. Slag, metal and temperature samples are taken at this time. The ladle refractories are pitch-bonded doloma. The ladle is then transferred to an operating CLU.

The doloma lined CLU has five bottom tuyeres (supplying H_2O, N_2, Ar and O_2) and a top lance supplying oxygen only. Maximum bottom flows utilised are 110 Nm^3/min and the top lance is utilised at 120 Nm^3/min. Decarburisation and reduction periods are grade dependent and range from 45 to 75 minutes with an average of 60 minutes. The top lance is utilised for approximately 11 to 15 minutes per heat dependent upon start temperature, heat building requirements and transfer chemistry. The CLU process is controlled by an Uddeholm Technology supplied process control model, with fixed and dynamic blowing options. Slag, metal and temperature samples are taken after reduction. Slag formers and alloying additions are made throughout the process and are highlighted below.

After decarburisation and reduction, the CLU is tapped into a pitch bonded doloma lined teeming ladle (Mag-C slag line), which is then transferred to the ladle rinsing station. The slag is then rabbled, leaving approximately 500 to 800Kg of CLU slag. A synthetic slag is added to enable further desulphurisation and inclusion entrapment. Alloying additions are made to specification, and the steel temperature and chemistry are homogenised before transfer to the continuous casting machine.

3.2 Analysis Procedure

This work utilises standard plant samples taken from the various processing areas. The bulk slag was milled to a 150µm particle size, then briquetted, and the chemistry was analysed with an XRF fluorescence method (ARL9800 wavelength dispersive instrument) to determine the oxide compositions. The standard deviation for oxides in the slag ranges between 0.1 and 1 wt% dependent upon the particular oxide (CaO = 0.9%, Al_2O_3 = 0.3%, MgO = 0.1%, SiO_2 = 1%). The S in the slag was analysed by means of a Leco CS200 instrument with a standard deviation of 0.004 wt%. The steel samples are ground on P80 grit Al_2O_3 paper and polished on P180 grit Al_2O_3 paper and analysed by means of the ARL9800 XRF technique. The standard deviation for S in the steel is ±0.001 wt%. The carbon was analysed by means of a Leco CS400 optical emission spectrometer with a relative accuracy of 0.003 wt%. The oxygen and nitrogen were analysed by means of a Leco T316 OES, with a standard deviation of ±20 ppm.

Plant sampling trials for slag samples in the past have indicated a 1 to 2% relative standard error for multiple samples taken at one occasion. These tests have only been conducted on liquid slags.

The Columbus Stainless laboratory is SABS 0259 accredited.

4. Discussion
4.1 CLU Slag Chemistries

The current philosophy behind slag former additions and practices are based on several criteria: refractory protection; desulphurisation; ease of metallic oxide reduction; processing speed; slag former chemistry and temperature control. The slag chemistry is therefore an optimisation process between competing requirements.

The aim CLU slags are close to lime saturation at 1720 ^{o}C and contain 11% MgO (Figure 1 shows the final aim chemistry on the CaO-MgO-SiO$_2$ slag system, point A)[15]. A fully lime saturated slag would require higher lime additions thus increasing processing time and would be crusty. The 11% MgO allows lower CaF$_2$ additions at or before reduction, due to its ability to flux CaO and SiO$_2$. (The mean CLU slags are shown in Table 1). The slag former additions are added at various stages in the process and are shown in Table 2. There are several reasons for this distribution of additions: slag former chemistry (Table 3), EAF transfer Si, temperature management and decarburisation efficiency.

The high levels of carbon in dolomite limits the window for additions time during the process, thus without decreasing the decarburisation efficiency and increasing processing time, the additions are made before 0.25% carbon is attained. The EAF transfer Si (average of 0.3wt%) requires neutralisation by lime and dolomite additions with an aim CaO/SiO$_2$ > 3, thus solidifying the slag completely during the initial stages of the blow with the top lance. This high CaO/SiO$_2$ level also ensures that the 1790°C (2CaO.SiO$_2$) eutectic in the CaO-MgO-SiO$_2$ system is not exceeded by the slag. (Note that normal bath processing temperatures are 1720 to 1740°C, but the top lance can generate temperatures in excess of 2000°C in localised areas.). Figure 1 shows the starting CLU slag chemistry as point B.

Lime, which has a lower carbon content than the dolomite, is used at reduction along with CaF$_2$ and FeSi. Low carbon heats (<0.010 wt%) utilise CaF$_2$ additions during decarburisation to limit carbon pick-up at reduction. Due to the high slag volumes and high CaO/SiO$_2$ ratio towards the end of decarburisaton, the CaF$_2$ is required to effectively flux the slag, to ensure it is liquid and reactive, for maximum desulphurisation and Cr recovery during reduction.

Figure 2 shows the CLU tap S levels vs. the start S levels for various grades produced. The mean sulphur levels from each stage in the process are listed in Table 4. The average reduction in sulphur from the start of CLU processing to tapping is 84.5%, by controlling the slag chemistry and additions practice. The scatter in Figure 2 for the tap S level is due to variations in additions during production. As will be seen in Figure 4, the final S is rarely above 0.005% which is the internal maximum.

4.2 Rinsing Station Slag Chemistries

The philosophy behind the rinsing station slag is a combination of several criteria: steel grade and customer requirements (0.003wt%S max. or Ti stabilised grades); temperature control (no heating facilities are available); refractory protection; and inclusion removal.

The aim and actual rinsing station slags are shown in Table 1. Aim slag chemistries are also recalculated and shown in the 4-component CaO-Al2O3-MgO-SiO2 quaternary phase diagram (Figure 3)[15]. The chemistries of the slag former additions utilised are shown in Table 3. It will be noted, that the calcium aluminate slag former is a pre-melted product and hence a relatively expensive source of alumina. This product is used due to its low melting point, rapid melting and consistent quality. The thermal reserve in the steel for melting slag former additions is limited, due to the CLU tap temperature of 1680 to 1700 ^{o}C and the aim tundish temperatures in the range of 1480 to 1520 ^{o}C (austenitic grades) and 1540 to 1560 ^{o}C (ferritic grades). Normally, metallic additions are in the range of 4.5 to 7.5 tons, which results in an average of 16 ^{o}C per ton of additions.

Slag formers are added in fixed ratios and in a set order after rabbling of 1 part CaF2:4 parts CA:1.5 parts Lime. The order of addition is critical, as the CLU slag remaining on the ladle after rabbling quickly stiffens, as the slag is completely lime saturated at 1640°C. The CaF$_2$ aids in fluxing the carryover slag, thereby allowing the rapid melting of the calcium aluminate, and finally dissolution of lime. The resultant slag is slightly below MgO saturation, but has a balanced CaO content, thus providing the refractory with some protection. Currently a high quality (low carbon containing) dolomite material is not locally available, to increase the MgO levels. A higher MgO content in the calcium aluminate is also not currently available. The slag former additions drop the steel temperature by 20 to 25 degrees, depending upon the mass of total addition (usually in the range of 650 Kg). This temperature drop is predictable and calculated by the rinsing station process control model.

The utilisation of such a slag has several benefits: absorbtion and retention of S due to a very high sulphur capacity; absorbtion of both alumina and titanium oxides; limited oxygen and nitrogen pick-up during rinsing; and insulation of the steel to some extent during casting. As the slag is liquid down to casting temperatures, the slag also allows easy penetration of lump, granule and wire additions during processing. The chemistry of the rinsing station slag is carefully chosen to allow higher CaO contents (CaF$_2$[16] increases the CaO solubility) and thus a higher CaO activity ($\mathbf{a}_{CaO}$). Addition of Al$_2$O$_3$[17] dilutes the SiO$_2$ content and thus it's activity, thereby further increasing the ($\mathbf{a}_{CaO}$). As a result, the slag has a substantially higher C$_S$ compared to the CLU slags[18].

During this work several slag-sampling trials were conducted and the mean analysis is presented in Table 1.

A comparison of the S level after tapping the CLU and the end of ladle rinsing is shown in Figure 4. Analysis of the plant data has indicated a mean decrease in S from tapping to the end of rinsing of 45 to 48% for 18% Cr steels (both austenitic and ferritic) and a 50% decrease for 12% Cr steels (ferritic only). As can be seen in Figures 2 and 4 the 0.003% and 0.001% S levels are achievable during CLU and rinsing station processing. The scatter is primarily due to lower slag former additions by the melters, in order to achieve increased throughput. The internal maximum S level of 0.005wt% is however, seldom exceeded, even with the lower slag former additions.

4.3 Sulphur Distribution

The L$_S$ calculations detailed in equations 12, 13 and 14 were applied to the CLU slags, with 2 conditions for Al$_2$O$_3$ activity. These were that $\mathbf{a}_{Al2O3} = 1$, i.e. where the equilibrium is with respect to the solid inclusion, and $\mathbf{a}_{Al2O3} < 1$ in the slag, using the data calculated by Ohta and Suito[9]. Figure 5 shows the 3 forms of L$_S$ versus the measured L$_S$ value for all heats (1 to 1 indicates L$_S$ measured = L$_S$ calculated). Some of the results indicated [Si] control, while others indicated [Al] control. For L$_{S2}$ calculations, the condition of $\mathbf{a}_{Al2O3} = 1$ was chosen to ensure Si control. The best fit is obtained with L$_{S2}$ (equation 13) which utilises the optical basicity modified for CaF$_2$, and the Si-SiO$_2$ equilibrium. Figure 6 shows the application of L$_{S4}$ (equation 15 for aluminium control)[9], which are the heats which indicated [Al] control of the oxygen. It must be noted that [Si] controlled the oxygen potential up to 0.008% [Al], and [Al] controlled the oxygen potential for 0.006 to 0.010% [Al]. The heats that fall within the 0.006 to 0.008% [Al] range are controlled by [Si], if [Si] > 0.65%. From figures 5 and 6 it is

apparent that the sulphur distribution ratio can be predicted from equation 13 for Si control and equation 15 for Al control.

Figure 7 shows the total and equilibrium oxygen values for the alloys investigated which had Al control of the oxygen equilibrium. It will be noticed that above 0.008 wt% total oxygen, there is a large deviation from the expected trend. This is probably due to oxidation of the samples during drilling, leading to high total oxygen levels or the presence of Al_2O_3 inclusions in the samples. (Final release samples utilise a different preparation technique, which minimises any possible contamination.) This deviation shows the importance of utilising the correct equilibrium oxygen calculations for determining L_S.

Figure 8 shows the application of equations 12, 13, 14 and 15 to the rinsing station slags. The calculated activity of Al_2O_3 [9] in the slag was used for all calculations. The heats with Al control were plotted using equation 15, and those with Si control using equations 12, 13 and 14. No real conclusion can be drawn with regards to which equation supplies the best fit, due to the limited sample size. By setting $\mathbf{a}_{Al2O3}$ to unity i.e. where the equilibrium is with respect to the solid inclusion, and utilising a fixed oxygen activity of $4*10^{-4}$, a reasonable fit of the data is possible for equation 13. This implies that the activity of SiO_2 or Al_2O_3, and hence equilibrium oxygen, do not follow the prediction of Ohta and Suito[9] for the particular metal-slag compositions investigated at the rinsing station.

The application of equation 15 was further investigated by considering the following equilibrium:

$$[Al] + \tfrac{3}{2} SiO_2(l) = \tfrac{3}{2}[Si] + Al_2O_3(s) \qquad (16)$$
$$\Delta G_{16}^o = \text{-164600} + 26.8\text{T [J/mol]}^{[9]}$$
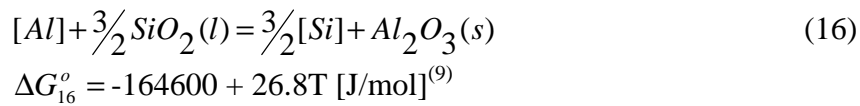
Minimum [Si] levels required to control the oxygen potential were calculated for $\mathbf{a}_{Al2O3} = 1$ and for $\mathbf{a}_{Al2O3} < 1$ [9] for the rinsing station slags. These are shown in Table 5, and indicate the potential for mixed control by Al or Si, when the minimum and actual [Si] values are close. Minimum values of $\mathbf{a}_{Al2O3}$ required for Si control were sample dependent, and are also shown in Table 5. The required $\mathbf{a}_{SiO2}$ for Si control at the calculated $\mathbf{a}_{Al2O3}$ [9] were included, for those heats where the Al was predicted to control the oxygen potential.

It is clear from these data that the control of [O] in the steel can swing from [Si] to [Al] and vice versa very easily, from small changes in the compositions of the steel or slag. In practice, the equilibrium involving Al_2O_3 in the slag, will play a role when a sufficient number of Al_2O_3 inclusions have been removed from the bulk steel to the slag or sidewalls (i.e. when the steel is no longer flooded with Al_2O_3 particles with an activity of 1). This is dependent on the amount of Al added in the bulk ferroalloys as impurities, either at reduction or in the ladle. Also, as proposed in references 5 and 7, [Al] may be locally controlling the oxygen potential at the slag-steel interface, rather than [Si] in the bulk steel.

It must be noted that at 1580 ^{o}C, the steels are predominantly controlled by the Si content of the steel, due to the low $\mathbf{a}_{SiO2}$, as shown in Figure 9. The large differences between the equilibrium oxygen and the total oxygen for the rinsing station samples (Figure 7), is due to the sample preparation technique or the presence of Al_2O_3 in the steel and that the steel in the ladle is not at equilibrium. In the work of Andersson et al[12], the large deviations in calculated

L_S versus measured L_S, were also noted prior to degassing in the ladle. After degassing, the steel was closer to equilibrium, hence allowing the successful application of a laboratory based technique to a plant environment. Oxygen probe (Celox) readings at the rinse station, have in the past indicated an oxygen level between 0.002 and 0.004 wt% in solution (grade dependent), which also indicates that the steel is not at the calculated equilibrium[9].

5. Conclusions

The application of various sulphur distribution ratios to both the CLU and rinsing station slags has been described yielding good predictions for CLU slags under Si and Al equilibrium control. The application of the sulphur distribution ratios to the rinsing station slags was not successful when utilising the current equilibrium calculations.

The key findings of this work are as follows:

- [S] levels of 0.003 wt% are achievable in the CLU with a single slag practice based on a detailed understanding of the process, slag chemistry, thermodynamics of desulphurisation and slag-refractory compatibility.

- The sulphur partition ratio L_S, can be modelled for the CLU slags by using equations for [Si] or [Al] control of the oxygen potential.

- A rinsing station aim slag chemistry of 20%Al_2O_3, 15%SiO_2, 7%MgO, 54.5%CaO and 3%CaF_2, allowed a reduction in sulphur of up to 50%; protection of the refractories and predictable temperature losses, for a total slag mass of only 1.5 Tons (650 Kg slag formers and 800 Kg CLU slag).

- Addition of a limited quantity of purpose designed slag of high C_S at the rinsing station, enables the achievement of 0.001wt% [S] in the steel. The rinsing station slag can also aid in the removal of Al_2O_3 inclusions, as it has a high capacity for absorbing Al_2O_3.

- The control of oxygen potential can be by either [Si] or [Al] in the steel, with the activities of the respective oxides estimated for the ladle slags. The results suggest that the species dictating the oxygen potential will change with processing time, or may depend on the localised equilibrium at the slag-metal interface. Stipulation of a fixed oxygen activity in the steel and $\mathbf{a}_{Al2O3} = 1$, were necessary to accurately predict the sulphur distribution ratio with rinsing station (ladle) slags. Further work is therefore required to measure the activities of Al_2O_3 and SiO_2, and C_S for these particular slags.

REFERENCES

1. D.J. Sosinsky and I.D. Sommerville: Metallurgical transactions B, Volume 17B, June 1986, pp331-337.
2. J.A. Duffy: Ironmaking and Steelmaking, 1990, Volume 17, No.6, pp.410-413.
3. J. Lehmann, H. Gaye, W. Yamada, and T. Matsumiya: Proc. 6th Int. Iron and Steel Congress 1990, Nagoya, ISIJ, pp256-263.
4. F.D. Richardson: Physical Chemistry of melts in Metallurgy, Volume 2, Academic Press, London, 1974.
5. R Inoue and H Suito: Steel Research 65, 1994, No. 10, pp.403-409.
6. F*A*C*T thermodynamic database. McGill University, Montreal, Canada.
7. L. Jonsson, Du Sichen and P Jonsson: ISIJ International, Volume 38 (1998), No. 3, pp.260-267.
8. H. Suito, H. Inoue and R. Inoue: ISIJ International, Volume 31, No.12, 1381-1388.
9. H Ohta and H Suito: Metallurgical Transactions B, Volume 29B, February 1998, pp.119-129.
10. T. Tsao and H.G. Katayama: Research Transactions ISIJ, 26 (1986), pp.717-723.
11. M.A.T. Andersson, P.G. Jonnson and MM Nzotta: ISIJ International, Volume 39 (1999), No. 11, pp.1140-1149.
12. H.B. Bell: Canadian Metallurgical Quarterly, Volume 20B, No. 2, pp.169-179, 1981.
13. M.M. Nzotta, Du Sichen and S. Seetharaman: ISIJ International, Volume 39 (1999), No. 7, pp.657-663.
14. M.M. Nzotta, Du Sichen and S. Seetharaman: Metallurgical Transactions b, Volume 30B, October 1999, pp.909-920.
15. Slag Atlas, 2nd edition, edited by Verein Deutscher Eisenhuttenleute (VDEh), 1995.
16. D.M. Edmunds and J. Taylor: J. Iron and Steel Institute, 210, (1972), pp.280-283.
17. H.R. Rein and J. Chipman: Trans. Metallurg. Soc., AIME, 233, (1965), pp415-425.
18. K. Susaki, M. Maeda and N. Sano: Met Trans B, Volume 21B, December 1990, pp.1081-1084.

Tables

Table 1: Slag chemistries under investigation. (All values wt%)

	%Al$_2$O$_3$	%SiO$_2$	%MgO	%Cr$_2$O$_3$	%FeO	%MnO	%TiO$_2$	%CaO	CaF2	%S
EAF aim	2	30	12	3	1	1	1	50		
EAF mean	2.74	29.99	11.5	3.8	.75	1.96	1.17	46.7	3	
CLU aim	1	30	11.5	1	0.5	0.5	0.5	53	3	
mean	0.944	31.737	11	1.382	.268	.332	.313	51.02	2.8	0.193
Rin aim	20	15	7					54.5	3	
Rin mean	19.04	16.02	6.68	.67	.28	.28	1.39	53.23	2.9	0.268

Table 2: Slag former additions during the CLU process. (All masses in Kg and carbon in wt%.) These are typical values for a 304HC heat.

Stage	Lime	Dolomite	CaF$_2$	%C
Upfront	3000	1500		1.5-2
Dec 2a	1300	2450		>0.25
Dec 3	500			0.080
Reduction	1000		700	0.030

Table 3: Basic raw Material Chemistries (wt%).

	C	MgO	CaO	CaF$_2$	Al$_2$O$_3$
Lime	0.02	1.9	91.7		
Dolomite	0.7	35	50		
CaF$_2$	0.05		4.2	85	
Calcium Aluminate	0.018		41.3		50.1

Table 4: Mean sulphur levels per station

Station	Mean S (wt%)	% Reduction
EAF	0.0226	
CLU	0.0035	84.5
Rinsing Station	0.0019	45.7

Table 5: Minimum Si requirements with varying activities of Al$_2$O$_3$ [9] from equation 16.

a_{Al2O3}	Min Si	a_{Al2O3}[9]	Min Si	Reqa_{SiO2}*	Reqa_{Al2O3}**	a_{SiO2}[9]	Actual Si
1	0.048	0.0233	0.584	0.0005	0.041	0.0007	0.48
1	0.036	0.0210	0.447		0.018	0.0009	0.53
1	0.045	0.0227	0.566	0.00097	0.026	0.0011	0.52
1	0.018	0.0159	0.283		0.007	0.0004	0.49
1	0.053	0.0210	0.699	0.00093	0.034	0.0012	0.50
1	0.060	0.0227	0.748	0.00105	0.035	0.0014	0.56

Req$\mathbf{a}_{SiO2}$* = required activity of SiO$_2$ for Si control of the oxygen potential in the steel whilst utilising the calculated $\mathbf{a}_{Al2O3}$[9].

Req$\mathbf{a}_{Al2O3}$** = required activity of Al$_2$O$_3$ for Si control of the oxygen potential in the steel whilst utilising the calculated $\mathbf{a}_{SiO2}$[9].

Appendix 1. Interaction Parameters used in the activity calculations

Values of f_i were calculated from the Taylor expansion for the weight percentage standard state i.e.

$$\log f_i = \sum_{j=2}^{m} e_i^j [\% j] + \sum_{j=2}^{m} r_i^j [\% j]^2 + \sum_{j,k=2}^{m} r_i^{j,k} [\% j][\% k] \text{ , where } j \neq k$$

j	i	e_i^j	(r_i^j)	Reference
C	O	-0.421		3
S	O	-0.133		1
P	O	0.07		1
Mn	O	-0.021		1
Si	O	-0.137		2
V	O	-0.3		1
Cu	O	-0.013		1
Co	O	0.008		1
Ti	O	-0.6		1
Mo	O	0.0035		1
Cr	O	-369/T - 0.137	0.0024 * % Cr$^{1.75}$	2
Ni	O	0.005		2
Al	O	-3.9		1
Nb	O	-0.14		1
B	O	-2.6		1
N	O	-0.14		3
O	O	-1750/T + 0.76		1
C	Si	0.25		2
S	Si	0.056		1
P	Si	0.11		1
Mn	Si	-0.0146		3
Si	Si	3910/T - 1.77		2
V	Si	0.025		1
Cu	Si	0.014		1
Co	Si	-		
Ti	Si	0.0396		4
Mo	Si	-		
Cr	Si	0		2
Ni	Si	0.0094	-0.00008	5

Al	Si	0.058		**1**
Nb	Si	-		
B	Si	0.2		**1**
N	Si	0.092		**3**
O	Si	-0.24		**2**
C	Al	0.091	-0.004	**1**
S	Al	0.03		**1**
P	Al	0.033		**3**
Mn	Al	-		
Si	Al	0.056	-0.0006	**1**
V	Al	-		
Cu	Al	-		
Co	Al	-		
Ti	Al	0.004		**4**
Mo	Al	-		
Cr	Al	0.04		**1**
Ni	Al	-0.0173	0.00021	**5**
Al	Al	0.04575	-0.001036	**4**
Nb	Al	-		
B	Al	-		
N	Al	$1650/T - 0.094$		**1**
O	Al	$-34740/T + 11.95$		**1**
C	S	0.11	0.0058	**1**
S	S	$233/T - 0.153$	-0.0009	**1**
P	S	0.29	0.0006	**1**
Mn	S	-0.026		**1**
Si	S	0.063	0.0017	**1**
V	S	-0.016		**1**
Cu	S	-0.0084		**1**
Co	S	0.0026		**1**
Ti	S	-0.072	0.0001	**1**
Mo	S	0.0027		**1**
Cr	S	$-94.2/T + 0.0396$		**1**
Ni	S	0.0037		**1**
Al	S	0.035	0.0009	**1**
Nb	S	-0.013	-0.0001	**1**
B	S	0.13	0.0074	**1**
N	S	0.0089		**1**
O	S	-0.27		**1**

References for Appendix 1

1. G.K. Sigworth, and J.F. Elliot. The thermodynamics of liquid dilute iron alloys. Met.Sci., 1974, Vol. 8, pp. 298-310.

2.   T.Toge and T. Watanabe. The deoxidation ability of silicon in molten stainless steel. Trans. ISIJ, Vol. 15, 1975, pp580-588.

3.   Steelmaking Data Sourcebook. The Japan society for the promotion of science. Gordon And Breach. New York. 1988.

4.   G. Yuanchang and W. Changzen. Met.trans. B (21B). 1990. p543-547

5.   Y. Li, R.Inoue and H.Suito. Measurement of aluminium or silicon activity in Fe-Ni (<30%) alloys using mullite and ZrO_2 based solid electrolyte galvanic cell. Steel Research, vol. 67, 1996, No.12.

Figures

Figure 1: SiO$_2$-MgO-CaO Ternary phase diagram[15]. Point A indicates the aim reduction slag. Point B indicates the start slag chemistry. Note that the CaF$_2$ addition at reduction will increase the area of the fully liquid field of the diagram.
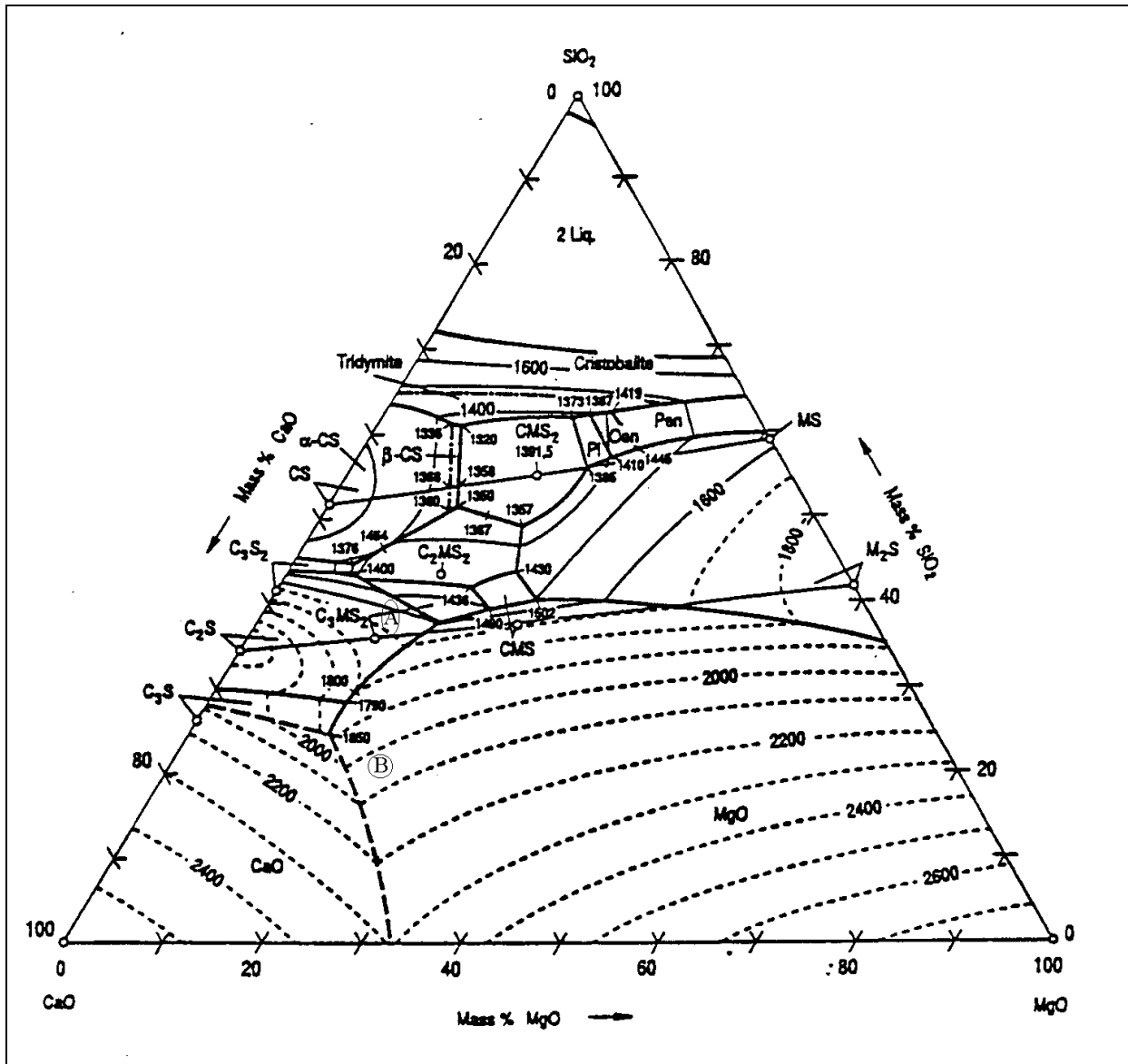
Figure 2: Tap CLU Sulphur level and EAF Tap Sulphur level. (V_S is the CLU slag analysis; the line indicates the mean final S level of 0.0035%.)
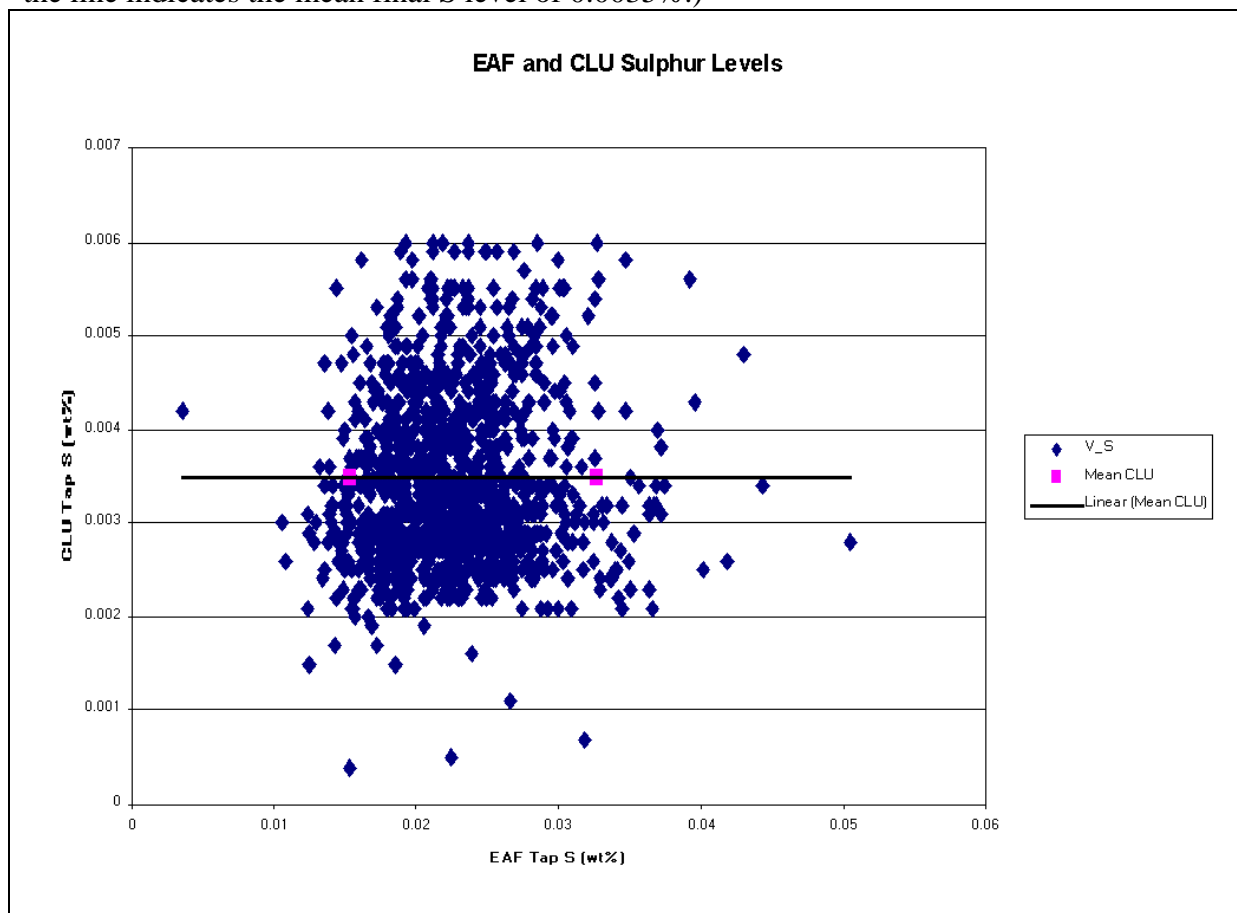
Figure 3: 20% Al_2O_3-CaO-SiO_2-MgO Quaternary phase diagram[15]. The shaded area indicates the aim slag chemistry. It must be noted that the CaF_2 addition increases the liquid field dramatically.
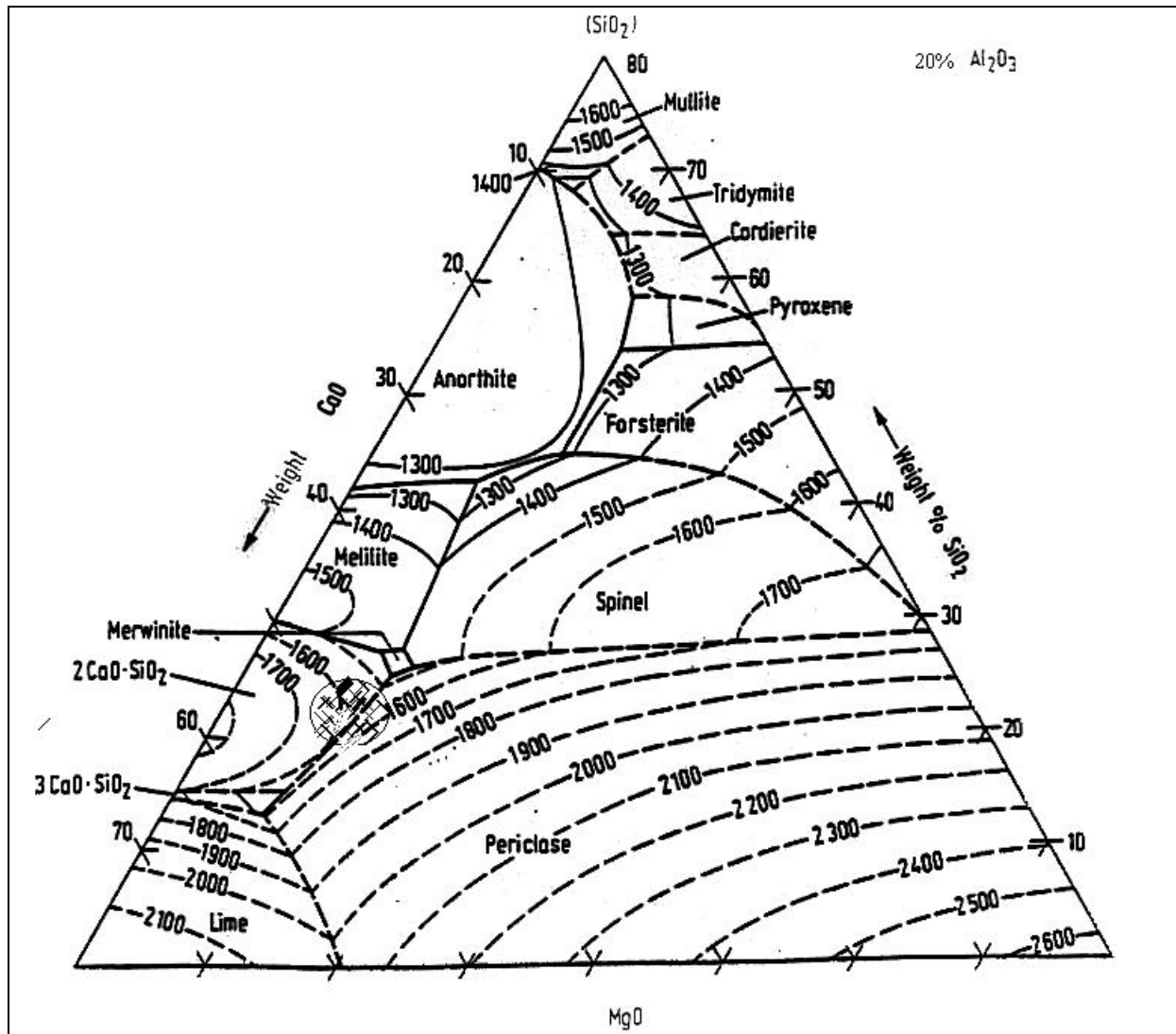
Figure 4: Tap CLU Sulphur levels vs. End Rinsing Sulphur levels. (L_S is the ladle sulphur measurement.)
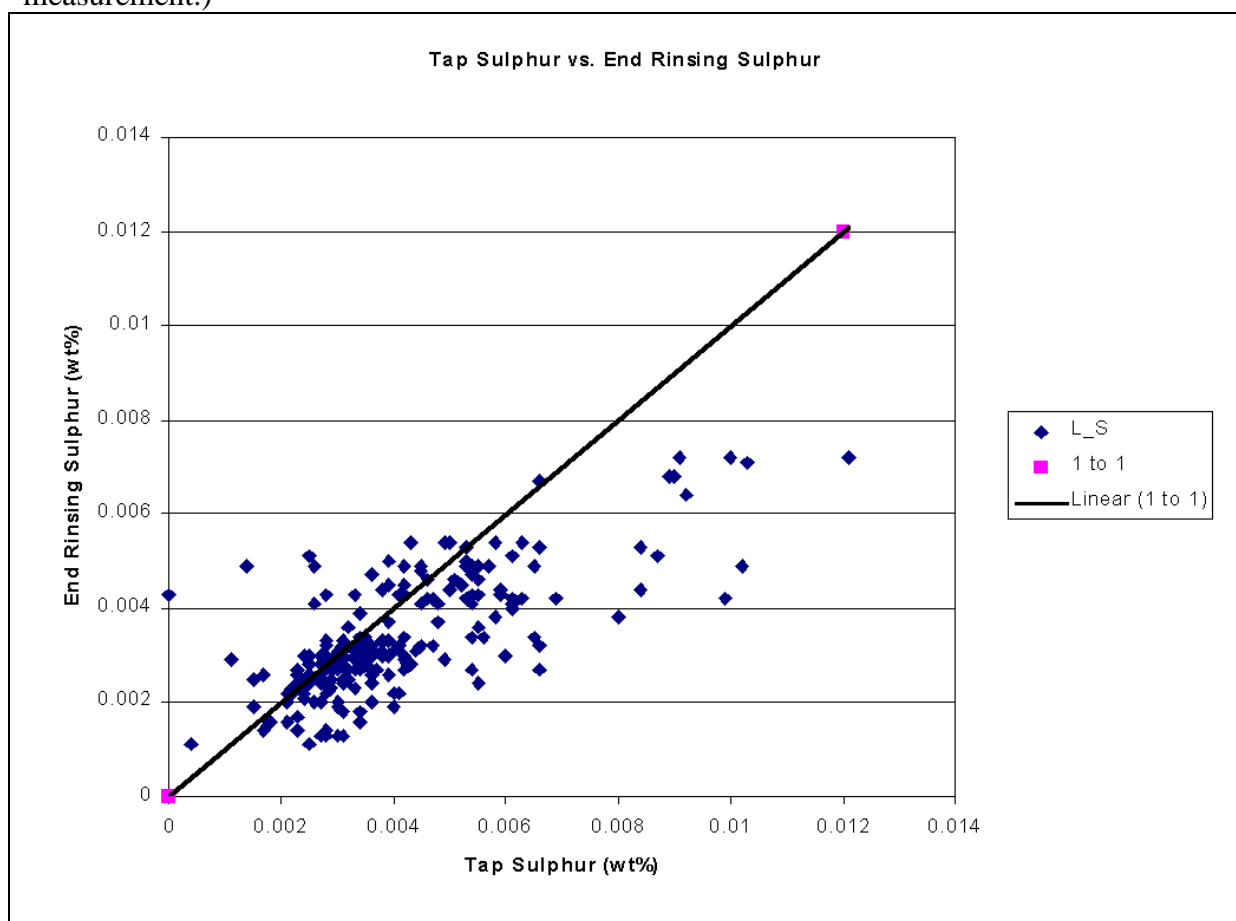
Figure 5: Application of LS equations to the CLU slags. LS1 = equation 12[1], LS2 = equation 13[2], LS3 = equation 14[5].
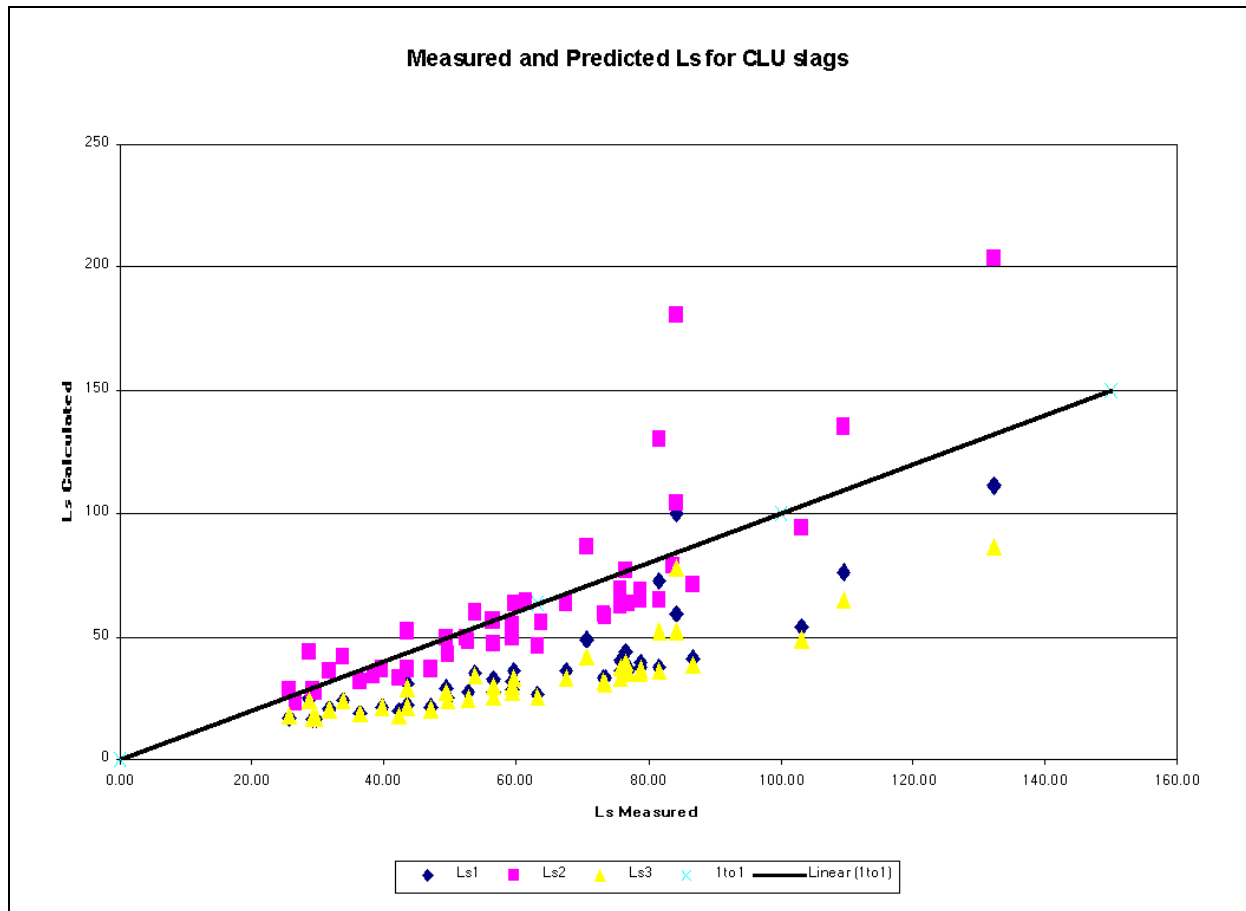
Figure 6: Application of LS equation 15[5] to the CLU slags.
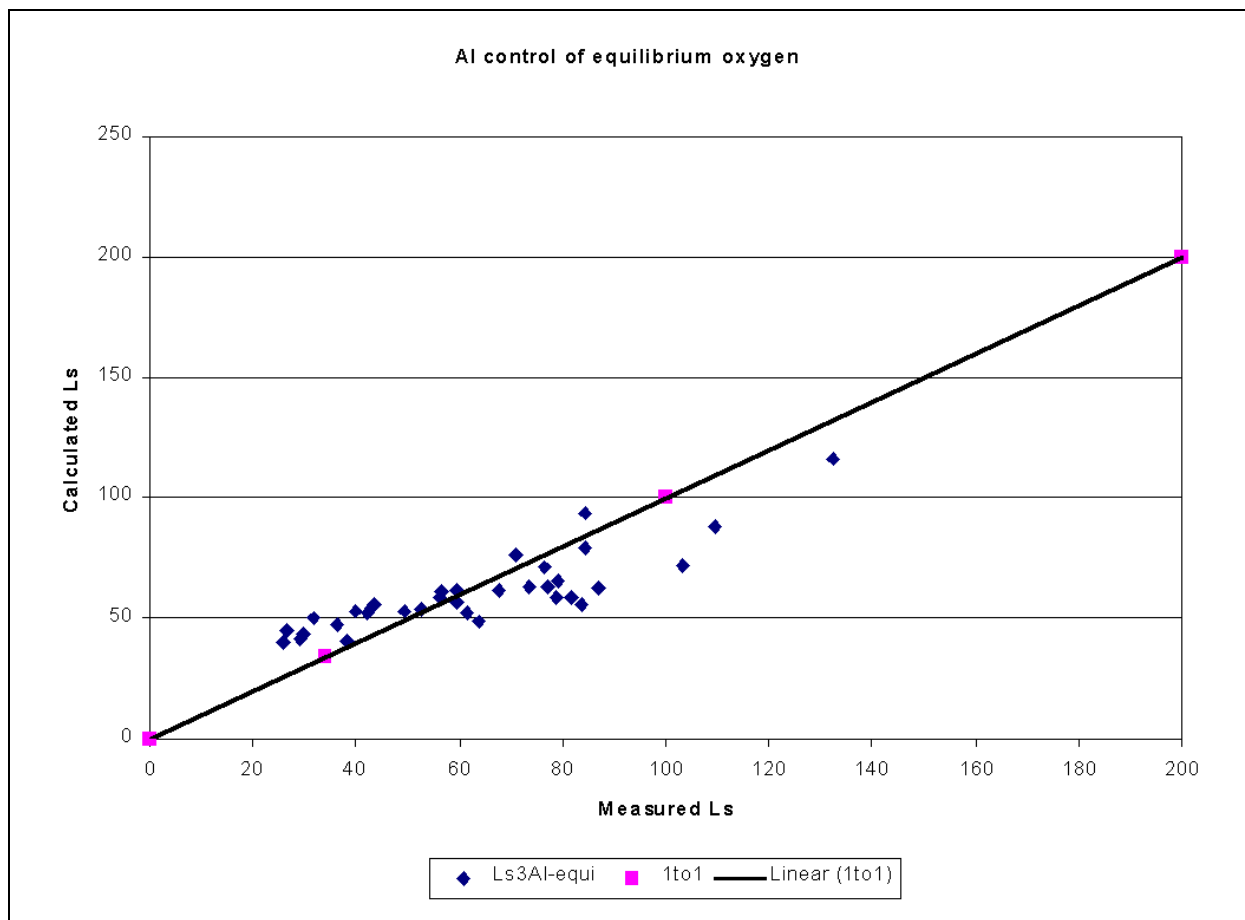
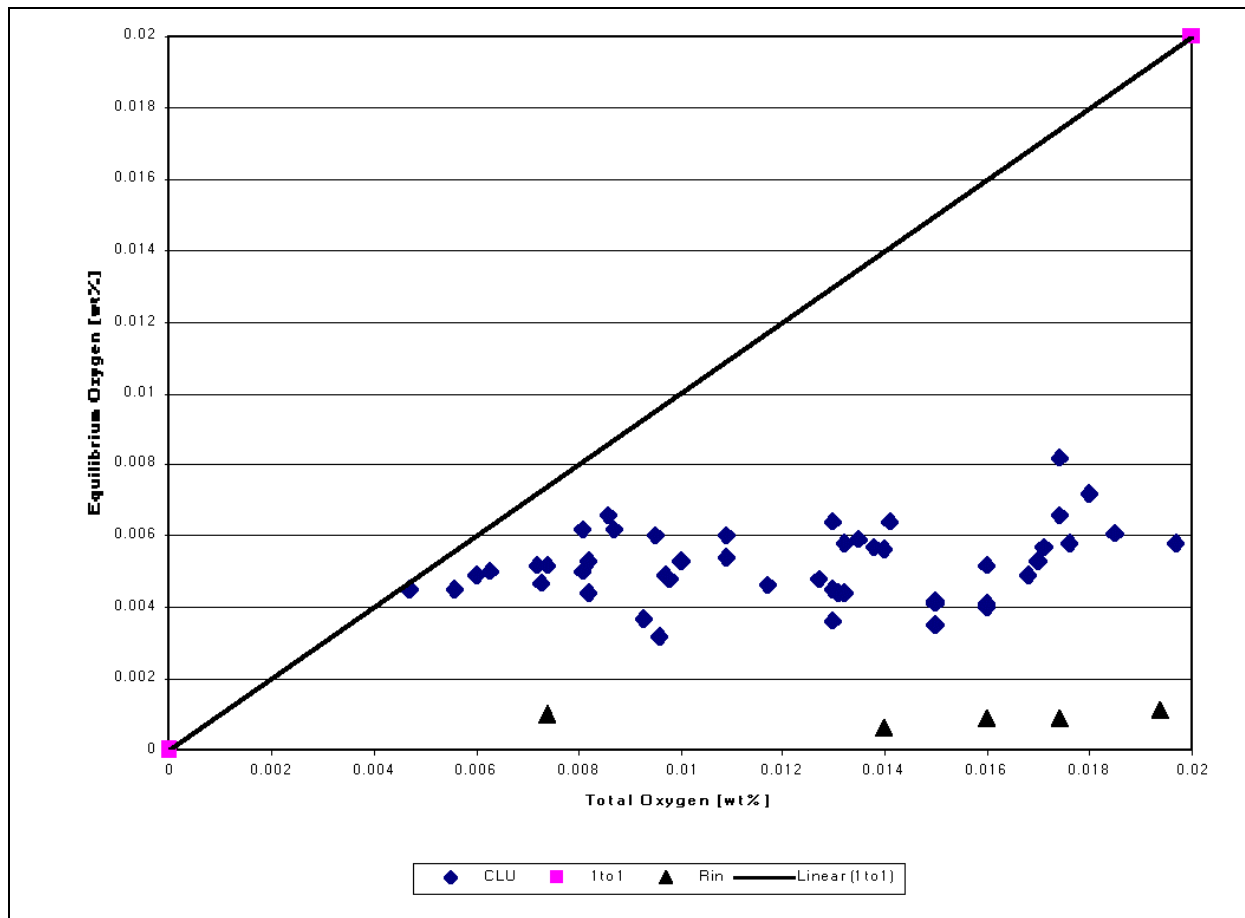Figure 7: Total oxygen versus equilibrium oxygen at the CLU and rinsing station.

Figure 8: Application of LS calculations for the rinsing station slags. LS1 = equation 12[1], LS2 = equation 13[2], LS3 = equation 14[5], LS3 Al-equi = equation 15[5]. Mod = a_{Al2O3} = 1 and fixed oxygen activity of $4*10^{-4}$
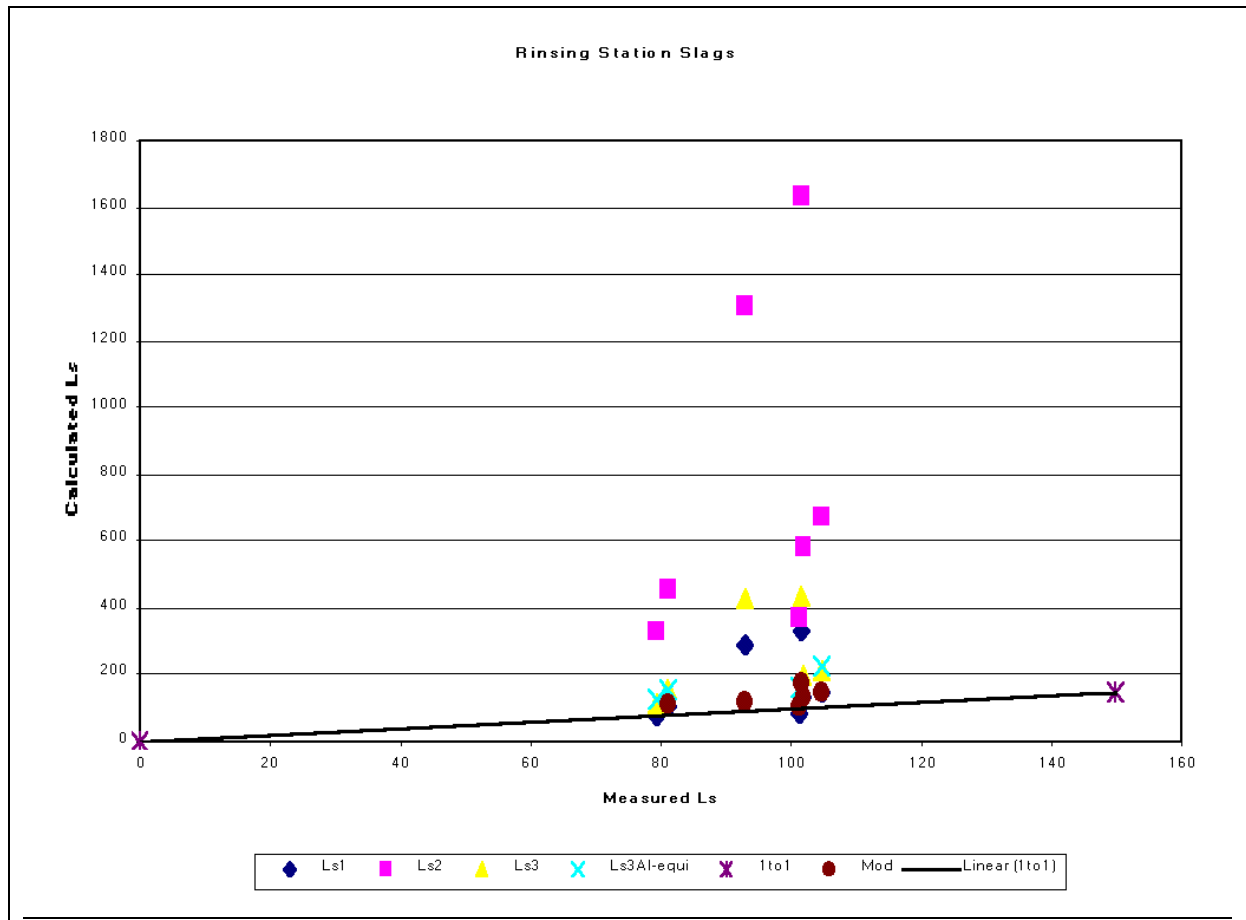
Figure 9: a_{SiO2} and a_{Al2O3} versus equilibrium oxygen for CLU and rinsing station slags.